

DOROTA ZIĘTEK*

DIFFUSED PHASE TRANSITION IN POLYCRYSTALLINE



ROZMYTA PRZEMIANA FAZOWA



Abstract

In this paper, the method of manufacturing solid solution $(\text{Ba}_{0.70}\text{Pb}_{0.30})(\text{Ti}_{0.70}\text{Sn}_{0.30})\text{O}_3$ (BP30TS30) is presented. Dielectric spectroscopy and scanning electron microscopy methods were applied to investigate the influence of doping by Pb and Sn on the physical properties of BaTiO_3 (BT). It is shown that Pb and Sn substitutions change the temperature of phase transitions, their character and the maximum value of electric permittivity.

Keywords: Ferroelectric ceramics, perovskite structure, barium titanate, diffused phase transition

Streszczenie

W artykule przedstawiono metodę otrzymywania stałego roztworu $(\text{Ba}_{0.70}\text{Pb}_{0.30})(\text{Ti}_{0.70}\text{Sn}_{0.30})\text{O}_3$ (BP30TS30). Badania przeprowadzone za pomocą spektroskopii dielektrycznej i skaningowej mikroskopii elektronowej miały na celu sprawdzenie wpływu domieszkowania jonami ołowiu i cyny na własności BaTiO_3 (BT). Wykazano, iż domieszki Pb i Sn zmieniają zarówno temperaturę przemian fazowych, ich charakter, jak i maksymalną wartość przenikalności elektrycznej.

Słowa kluczowe: ceramika ferroelektryczna, struktura perowskitu, tytanian baru, rozmyta przemiana fazowa

* M.Sc. Eng. Dorota Ziętek, Institute of Physics, Pedagogical University, Cracow.

1. Introduction

Perovskite type ferroelectric materials have many technical applications. They are very popular due to the variety of their physical properties. The main advantages of these kinds of materials are high values of electric permittivity, polarization, electromechanical coefficients and short switching times. The simplest structure and composition among perovskite type (ABO_3) ferroelectrics has barium titanate $BaTiO_3$ (BT). Moreover, it is the most studied ferroelectric material in recent times [1]. Figure 1 shows the cubic structure of BT, however, depending on the temperature, this material can exist in four different crystalline phases.

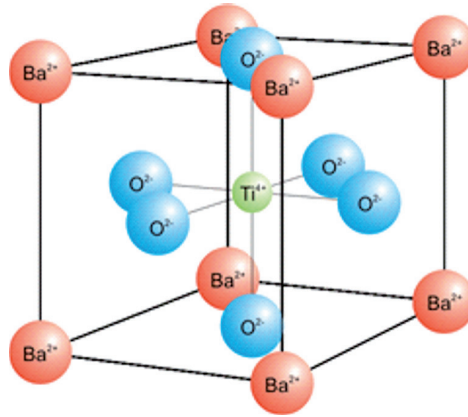


Fig. 1. Cubic structure of $BaTiO_3$

There are three phase transitions which can be observed during the cooling of $BaTiO_3$ [2]:

- $T_c = 403$ K transition from cubic phase ($Pm\bar{3}m$) to tetragonal phase ($P4mm$),
- $T_1 = 288$ K transition from tetragonal phase to orthorhombic phase II ($Amm2$),
- $T_2 = 183$ K transition from orthorhombic phase to rhombohedral phase ($R\bar{3}m$).

The cubic phase is paraelectric, but other phases are ferroelectric. Many kinds of solid solutions with various technical applications can be obtained by doping BT with different ions. The physical properties of these solutions depend on the substitution type and its concentration. One of the most important applications of perovskite type ferroelectric materials is FRAM (ferroelectric random access memory) made from thin films of PZT. This kind of memory has many advantages such as: low power usage; fast write performance; a huge number of write-erase cycles. PZT ceramics [3] might also be used in the production of micro-switches, different kinds of sensors, components of piezoelectronics, electromechanical transducers, ultrasound generators, high voltage transformers and echo-sounders [4]. Other electronic components are multilayer capacitors based on BT.

BT can be doped by Pb and Sn ions. Earlier studies of $PbBaTiO_3$ solid solution showed that an increase of Pb concentration leads to an increase in the paraelectric – ferroelectric (PE-FE) phase transition temperature [5]. In the case of $Ba(Ti_{1-y}Sn_y)O_3$, an increasing Sn

concentration causes a decrease of the phase-transition temperature value [6-11]. It is expected, while investigating BP30TS30, that both of the substitutions have an influence on its physical properties. An influence of substitutions in sublattices A and B was observed in compounds based on BT such as $(\text{Ba}_{0.90}\text{Sr}_{0.10})(\text{Ti}_{1-y}\text{Sn}_y)\text{O}_3$, $(\text{Ba}_{1-x}\text{Sr}_x)(\text{Ti}_{1-x}\text{Zr}_x)\text{O}_3$ [12], $\text{Ba}(\text{Ti}_{1-2x}\text{Fe}_x\text{Nb}_x)\text{O}_3$, $\text{Ba}(\text{Ti}_{1-x}\text{Hf}_x)\text{O}_3$ [13]. This influence also appears in solutions obtained by a mechanochemical method [14, 15].

2. Experimental Method

Polycrystalline samples of BT and BP30TS30 were prepared by using synthesis from the following powders: BaC_2O_4 , PbC_2O_4 , TiO_2 and SnO_2 . The purity of these reagents was 99.99%. Appropriate amounts of the components were grained in a ball mill for 2 hours. The mixture was then dried and a sample was formed using a tablet maker, under an uniaxial pressure of 0.3 GPa. Tablet synthesis was made in Nabertherm L 5/13/B180 muffle stove at 1273 K for 1 hour. The samples were then re-milled, formed and sintered at 1573 K for 1 hour. The obtained disc-like pellets, with a diameter of 8 mm and thickness ranging from 1.5 mm to 2 mm, were then covered with silver electrodes.

Microstructural investigations of BT and BP30TS30 samples were made using the Jeol JSM-6610F scanning electron microscope. The composition of the samples was checked using the EDS (Energy-Dispersive X-Ray Spectroscopy) analyzing method. Dielectric measurements were carried out using an Alpha-AN High Performance Frequency Analyzer system together with a cryogenic temperature control system – Quatro Cryosystem and WinDETA Novocontrol software. Dielectric properties of the samples were measured in a wide frequency range from 0.1 Hz to 10 MHz. Nitrogen gas was used as a heating and cooling agent.

3. Results and Discussion

Figures 2–4 show SEM photomicrographs of BT and BP30TS30 samples.

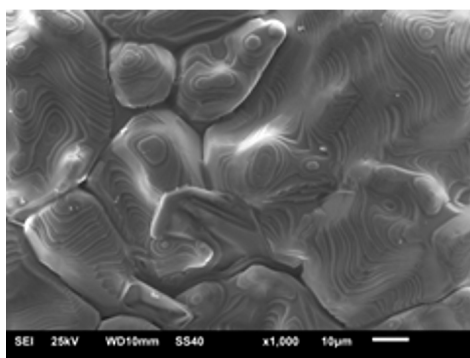


Fig. 2. SEM image for BT

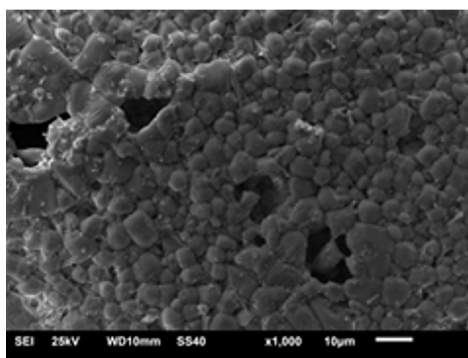


Fig. 3. SEM image for BP30TS30

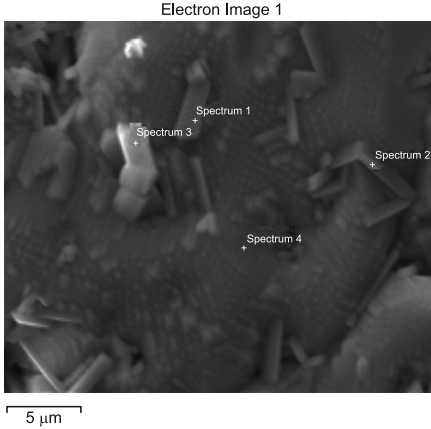


Fig. 4. SEM image for BP30TS30

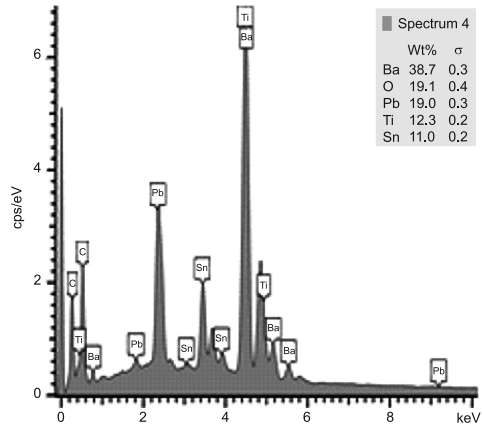


Fig. 5. EDS spectrum for BP30TS30

One can observe that grains in BP30TS30 are much smaller than grains in pure BT (Fig. 2, 3). A structure of BP30TS30 with well-defined grain borders can be clearly seen in the SEM photomicrograph (Fig. 4).

The EDS analysis results, shown in Figure 5, confirm that BP30TS30 sample contains only: Ti, Ba, Pb and Sn atoms. Carbon sputtered on the sample surface during its preparation can also be seen in EDS spectrum because of the specimen preparation mode.

Fig. 6 and 7 show the temperature dependence of the real part of electric permittivity for BT and BP30TS30 respectively.

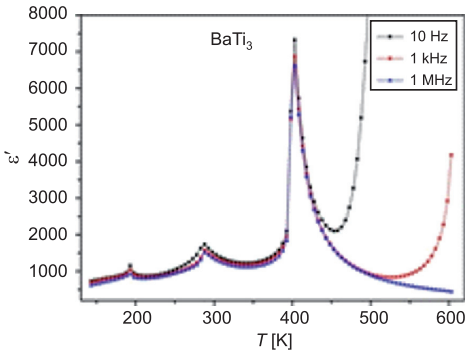


Fig. 6. Temperature dependence of the real part of electric permittivity for BT

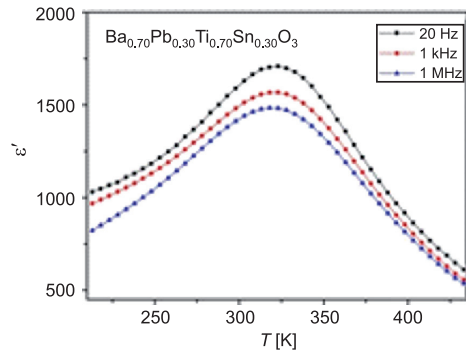


Fig. 7. Temperature dependence of the real part of electric permittivity for BP30TS30

In Fig. 6 there are three strong $\epsilon'(T)$ peaks corresponding to the BT structural transitions which were described earlier. At 403 K, one can see a sharp phase transition from the paraelectric phase to the ferroelectric phase. The further lowering of the temperature shows two different phase transitions at 288 K and 188 K. In the case of BP30TS30, one can notice only one broad peak at about 320 K. In BP30TS30, containing the same percentage

value of both Sn and Pb atoms, there is a shift of the PE-FE transition temperature to lower temperatures than in BT. This means that an influence of Sn ions on the phase transition character is stronger than Pb ions. The observed temperature T_m , corresponding to the maximum value of the real part of permittivity ϵ_m , does not depend on the frequency of the applied electric field. It indicates rather diffused phase transition. The degree of phase transition diffusion can be derived from the following expression:

$$\frac{1}{\epsilon} \cdot \frac{1}{\epsilon_m} = A(T - T_m)^\gamma \quad (1)$$

where:

- ϵ – the real part of electric permittivity,
- ϵ_m – the maximum value of the real part of electric permittivity,
- A – a constant (for $\gamma = 1$ an inverse of the Curie-Weiss constant/coefficient),
- T – a temperature,
- T_m – the temperature of occurring the maximum value of electric permittivity,
- γ – a coefficient with value from 1 to 2, a value close to 1 denotes sharp phase transition, but close to 2 denotes diffused phase transition.

In order to determine a gamma coefficient value, a logarithm of both sides of the equation (1) should be taken:

$$\log\left(\frac{1}{\epsilon} - \frac{1}{\epsilon_m}\right) = \log A + \gamma \log(T - T_m) \quad (2)$$

When $\log\left(\frac{1}{\epsilon} - \frac{1}{\epsilon_m}\right)$ is plotted as a function of $\log(T - T_m)$, the gamma coefficient is a sloping straight line.

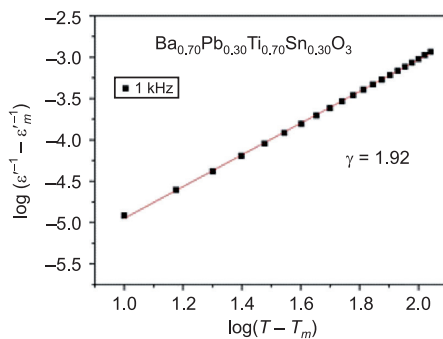


Fig. 8. A dependence of $\log\left(\frac{1}{\epsilon} - \frac{1}{\epsilon_m}\right)$ from $\log(T - T_m)$ for BP30TS30

The obtained value of the gamma coefficient is 1.92, so it is close to 2. This means that the phase transition in BP30TS30 is strongly diffused.

4. Conclusions

Experimental results confirmed that non-ferroelectric Sn ions in sublattice B have a very strong destructive influence on the created crystallographic structure. Ferroelectric Pb ions in sublattice A had a very small influence on crystallographic structure. Doping BT by the same amount of Sn substitutions leads to a strongly diffused phase transition across a wide range of temperature. This fact is important for designing devices with stable values of dielectric properties across a wide range of temperature.

The author would like to thank Prof. Czesław Kajtoch and Dr. Wojciech Bąk for their helpful discussions.

References

- [1] Kajtoch C., *Dilatometrische und dielektrische Anomalien bei den Phasenumwandlungen in $Ba(Ti_{1-x}Sn_x)O_3$* , Ann. Physik, vol. 2, 1993, 335-338.
- [2] Surowiak Z., *Elektroceramika ferroelektryczna*, Wydawnictwo Uniwersytetu Śląskiego, Katowice 2004.
- [3] Zarycka A., Zachariasz R., Czerwiec M., Ilczuk J., *Struktura i właściwości elektryczne ceramiki PZT otrzymywanej metodą zolowo-żelową*, Ceramika/Ceramics, 2005. Papers of the Commission on Ceramic Science, Polish Ceramic Bulletin Polish Academy of Science, Kraków Division, Polish Ceramic Society.
- [4] Nogas-Ćwikiel E., *Otrzymywanie proszków ceramicznych do kompozytów ceramiczno-polimerowych dla detektorów piroelektrycznych*, Uniwersytet Śląski, Katowice 2012.
- [5] Mitsui T., Marutake M., Sawaguchi E., *Landolt-Bornstein Numerical Data and Functional Relationships in Science and Technology*, Group III, Vol. 9, Springer-Verlag Berlin-Heidelberg-New York, 197.
- [6] Bąk W., Kajtoch C., Starzyk F., *Dielectric properties of $BaTi_{1-x}Sn_xO_3$ solid solution*, Materials Science and Engineering B100, Vol. 9, 2003, 9-12.
- [7] Kajtoch C., *Dielectric properties of $Ba(Ti_{1-x}Sn_x)O_3$ ceramics in the paraelectric phase*, Ceramics International, Vol. 37, 2011, 387-391.
- [8] Kajtoch C., Bak W., Garbarz-Glos B., *Study of the phase transition in polycrystalline $(Ba_{0.90}Pb_{0.10})(Ti_{0.90}Sn_{0.10})O_3$* , Condensed Master Physics, 2014.
- [9] Kajtoch C., *Time dependences of dielectric constant in $BaTi_{0.95}Sn_{0.05}O_3$* , Ferroelectrics, Vol. 133, 1992, 193-198.
- [10] Kajtoch C., *Dipolar polarization in $Ba(Ti_{1-x}Sn_x)O_3$* , Ferroelectrics, Vol. 172, 1995, 465-468.
- [11] Kajtoch C., *Glass-like transformation in $Ba(Ti_{0.70}Sn_{0.30})O_3$* , Ferroelectrics, Vol. 192, 1997, 335-337.
- [12] Kajtoch C., Bąk W., Garbarz-Glos B., Stanuch K., Tejchman W., Mroczka K., Czeppe T., *Influence of Sr and Zr substitution on dielectric properties of $(Ba_{1-x}Sr_x)(Ti_{1-x}Zr_x)O_3$* , Ferroelectrics 2014.
- [13] Garbarz-Glos B., Bąk W., Molak A., Kalvane A., *Microstructure, calorimetric and dielectric investigation of hafnium doped barium titanate ceramics*, Phase Transitions, 86, 2013, 917-925.

- [14] Dulian P., Bąk W., Wieczorek-Ciurowa K., Kajtoch C., *Controlled mechanochemical synthesis and properties of a selected perovskite-type electroceramic*, Materials Science Poland, Vol. 31(3), 2013, 462-470.
- [15] Dulian P., Wieczorek-Ciurowa K., Bąk W., Kajtoch C., *Możliwości wytwarzania zaawansowanej elektroceramiki na bazie tytanianu baru metodą mechanochemiczną*, Czasopismo Techniczne (Technical Transactions), Wyd. Politechniki Krakowskiej, Vol. 9-M/2012, Z. 26, 57-65.